Electrochemistry
The Electrochemical Society of Japan
Received: July 23, 2022
Accepted: August 20, 2022
Published online: October 31, 2022
Issued: October 31, 2022
https://doi.org/10.5796/electrochemistry.22-66088
https://doi.org/10.50892/data.electrochemistry.21357846
Comprehensive Paper
Electrochemistry, **90(10)**, 102002 (2022)

The 66th special feature
"Novel Aspects and Approaches to Experimental Methods for Electrochemistry"

Electrode Potentials Part 2: Nonaqueous and Solid-State Systems†

Jinkwang HWANG,[a,††,§] Takayuki YAMAMOTO,[b,††,§] Atsushi SAKUDA,[c,††,§] Kazuhiko MATSUMOTO,[a,*,§] and Kohei MIYAZAKI[d,§]

[a] *Graduate School of Energy Science, Kyoto University, Yoshida-Honmachi, Sakyo-ku, Kyoto 606-8501, Japan*
[b] *Institute of Advanced Energy, Kyoto University, Gokasho, Uji, Kyoto 611-0011, Japan*
[c] *Graduate School of Engineering, Osaka Metropolitan University, 1-1 Gakuen-cho, Naka-ku, Sakai, Osaka 599-8531, Japan*
[d] *Graduate School of Engineering, Kyoto University, Nishikyo-ku, Kyoto 615-8510, Japan*

* *Corresponding author: k-matsumoto@energy.kyoto-u.ac.jp*

ABSTRACT

This comprehensive paper, Electrode Potentials Part 2, is a continuation of Electrode Potentials Part 1: Fundamentals and Aqueous Systems. Determining the electrode potential is crucial for understanding the nature of the electrochemical properties of materials or systems; however, an accurate evaluation of the potential of a target electrode has always been a challenge. The electrode potential can be used to predict the reaction mechanisms in electrochemistry and can be directly applied to the study of electrochemical applications. This paper introduces the methodologies and strategies for measuring electrode potentials in nonaqueous and solid-state electrolytes, including organic solvent electrolytes, ionic liquid electrolytes, and oxide and sulfide solid electrolytes. Experimental details are described for basic to state-of-the-art strategies, focusing on practical methods and know-how.

Keywords : Electrode, Electrolyte, Nonaqueous Electrolyte, Solid-state Electrolyte

1. Introduction

The demand for electrochemical energy storage systems, such as secondary batteries and supercapacitors, increases with each passing year.[1,2] "Organic electrolytes" (organic solvents containing ionic species), have become standard for secondary batteries. Additionally, "ionic liquids" (liquid state salts consisting solely of cations and anions)[3–5] and "solid-state electrolytes" (oxides, sulfides, and polyanions)[6–9] are attracting more attention as promising electrolytes for next-generation batteries with high safety and performance.[10–12] However, measuring the precise potential of an electrode in these electrolytes has always been a challenge.

This comprehensive paper is a continuation of Electrode Potentials Part 1: Fundamentals and Aqueous Systems. Part 1 covers the fundamentals of electrode potentials based on their thermodynamic background with related materials and discusses the issues with electrode potentials in aqueous systems (potential–pH diagram, potential windows, practical reference electrodes, and mixed potentials). Part 2 focuses on the methodologies and strategies for measuring electrode potentials in nonaqueous and solid-state electrolytes. The first section of this paper discusses the general properties of common reference electrodes in nonaqueous electrolytes and their experimental and preparation methods. The second section introduces the concept of advanced reference electrodes using metal alloys and two-phase insertion-type compounds. The final section presents the experimental strategies and methods for measuring the electrode potential in a solid-state electrolyte. Detailed slides for each section are provided in the Supplementary Material.

2. Nonaqueous Systems

2.1 Common reference electrodes

Reference electrodes utilizing the Ag^+/Ag redox couple (hereafter "Ag reference electrode") are widely applied for electrochemical measurements in nonaqueous systems due to their high stability and easy handling.

$$Ag^+ + e^- \rightleftharpoons Ag \quad (1)$$

The Ag reference electrode is typically composed of a polished silver wire and a reference electrolyte containing a silver salt dissolved in a certain solvent. To avoid the outflow of silver species into the electrolyte to be measured (main electrolyte), the electrolyte used for the reference (reference electrolyte) is separated by a glass tube equipped with porous glass at one end as the liquid junction between the main and reference electrolytes. Figure 1 shows a schematic illustration of selected electrodes for electrochemical measurements. Single-junction and double-junction reference electrodes are commercially available. A single-junction glass tube is often used; however, a double-junction glass tube is recommended for long-term measurements. As mentioned in Section 2.5 of Electrode Potentials Part 1, a liquid junction potential appears at

†This paper constitutes a collection of papers edited as the proceedings of the 51st Electrochemistry Workshop organized by the Kansai Branch of the Electrochemical Society of Japan.
††These authors contributed equally to this work.
§ECSJ Active Member

K. Matsumoto orcid.org/0000-0002-0770-9210
K. Miyazaki orcid.org/0000-0001-5177-3570
J. Hwang orcid.org/0000-0003-4800-3158
T. Yamamoto orcid.org/0000-0003-3553-3272
A. Sakuda orcid.org/0000-0002-9214-0347

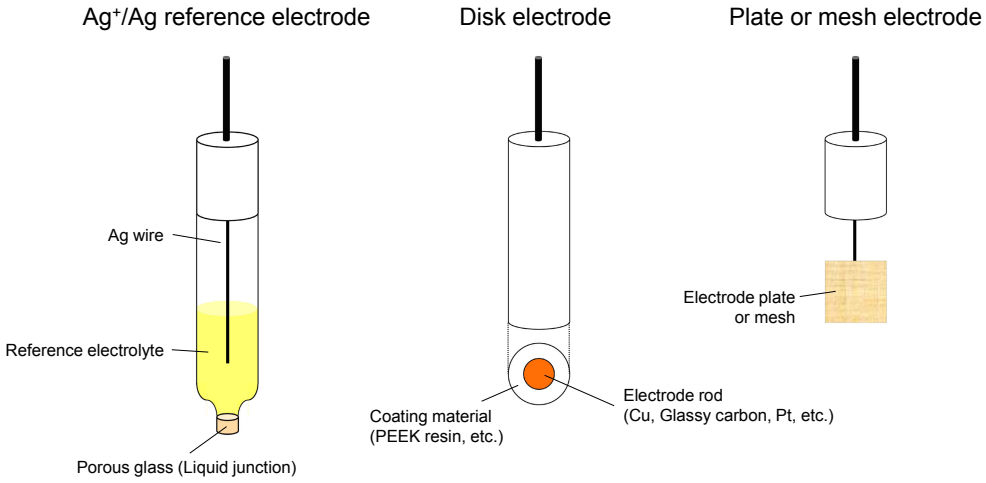

Figure 1. Schematic illustrations of selected electrodes for electrochemical measurements.

the junction of two different electrolytes. When it is difficult to use an appropriate salt bridge for examining the system, the liquid junction potential can be effectively eliminated by preparing reference electrolytes containing ionic species and/or solvents that are common to the main electrolytes. In addition, it is desirable to use a small-sized working electrode to reduce IR drop. To prevent the counter electrode from affecting the performance of the working electrode, the size of the counter electrode should be sufficiently larger than that of the working electrode. Migration of the reaction products at the counter electrode (e.g. by electrolyte decomposition) may sometimes affect the current behavior of the working electrode, which is needed to be taken into consideration.

Electrochemical measurements using Ag reference electrodes are both useful and convenient. However, the universality of the obtained potentials should be considered when comparing the results from various systems, because the Ag^+/Ag redox potential is known to significantly depend on the solvent.[13,14] According to the IUPAC recommendation,[15] the ferrocenium/ferrocene (Fc^+/Fc) redox couple is the universal standard because the Fc^+/Fc potential is considered to be independent of solvents owing to their bulkiness. The potential difference in various systems can be discussed on a common scale with the introduction of the Fc^+/Fc redox couple.

$$Fc^+ + e^- \rightleftharpoons Fc \tag{2}$$

After the desired electrochemical experiments are completed, ferrocene is dissolved in the main electrolyte, and its redox behavior is measured by cyclic voltammetry. The resulting Fc^+/Fc formal potential is used for the potential calibration. The principles and procedures are as follows.

In general, assuming a cyclic voltammetric measurement for a reversible reaction, the potential difference (ΔE_p) between anodic (E_{pa}) and cathodic (E_{pc}) peaks is expressed as follows:[16]

$$\Delta E_p = E_{pa} - E_{pc} = \frac{\Delta \widetilde{E}_p}{n} \tag{3}$$

where n is the number of electrons involved in the reaction and $\Delta \widetilde{E}_p$ is the potential difference of one-electron reaction. The $\Delta \widetilde{E}_p$ value varies slightly with the switching potential and is ideally 57.0 mV, practically in the range of 58–60 mV at 298 K. When the obtained $\Delta \widetilde{E}_p$ is close to these values, the reaction can be treated as a reversible reaction. In the case of the linear diffusion on a planar electrode, the half-wave potential corresponding to the half of the diffusion-limited current ($E^r_{1/2}$) is expressed as follows:

$$E^r_{1/2} = E^{\circ\prime} + \frac{RT}{nF} \ln \sqrt{\frac{D_R}{D_O}} \tag{4}$$

where $E^{\circ\prime}$, R, T, and F are the formal potential, gas constant, temperature, and Faraday constant, respectively. D_O and D_R are the diffusion coefficients of the oxidized and reduced forms of the reaction. On the assumption of $D_O = D_R$, the formal potential can be approximated as the average of the anodic and cathodic peak potentials.

$$E^{\circ\prime} = E^r_{1/2} \approx \frac{E_{pa} + E_{pc}}{2} \tag{5}$$

Then, the potentials measured using the Ag reference electrode can be calibrated to those with respect to the Fc^+/Fc redox potential ($E_{vs.\ Fc^+/Fc}$) using the following simple equation.

$$E_{vs.\ Fc^+/Fc} = E_{vs.\ Ag^+/Ag} - E^{\circ\prime}(Fc^+/Fc) \tag{6}$$

where $E_{vs.\ Ag^+/Ag}$ is the measured potential using the Ag reference electrode and $E^{\circ\prime}(Fc^+/Fc)$ is the formal potential of the Fc^+/Fc redox couple for the Ag reference electrode. Additionally, the diffusion coefficient of the reduced form (ferrocene in Eq. 2) is calculated using the following equation:[17]

$$i_{pa} = 0.4463 \sqrt{\frac{n^3 F^3}{RT}} C_R \sqrt{D_R v} \tag{7}$$

where i_{pa} is the anodic current density, C_R is the concentration of the reduced form in the bulk electrolyte, D_R is the diffusion coefficient of the reduced form, and v is the scan rate of cyclic voltammetry.

It should be noted that the reversible systems involved with multielectron reactions ($n \geq 2$) usually show the deviation from the theory mentioned above because the Eqs. 3, 4, and 7 can be applied only for one-step n-electron reaction. Since most of multielectron reactions are practically composed of n-step one-electron reactions, the statistical (entropic) factors should be considered for calculation of the standard potentials.[16,18] Assuming the systems of n equivalent, independent, and reversible active centers for one-electron transfer having the same standard potentials ($E^{\circ\prime}$), the entropic factor leads to the following equation for the redox potential of the jth one-electron transfer step ($E^{\circ\prime}_j$).[18]

$$E^{\circ\prime}_j = E^{\circ\prime} - \frac{RT}{F} \ln\left(\frac{j}{n-j+1}\right) \tag{8}$$

Then, the potential difference between 1st and nth redox reactions is obtained as follows:

$$\Delta E^{\circ\prime} = E^{\circ\prime}_n - E^{\circ\prime}_1 = -\frac{2RT}{F} \ln n \tag{9}$$

Table 1. Standard redox potentials (V) of $H^+/\frac{1}{2}H_2$, Li^+/Li, Na^+/Na, K^+/K, and Ag^+/Ag in different solvents.[14]

Solvent*	$H^+/\frac{1}{2}H_2$	Li^+/Li	Na^+/Na	K^+/K	Ag^+/Ag
Water	0.000	−3.040	−2.714	−2.936	0.799
PC	0.52	−2.79	−2.56	−2.88	0.99
MeCN	0.48	−2.73	−2.56	−2.88	0.56
EtOH	0.12	−2.93	−2.57	−2.77	0.85
DMF	−0.19	−3.14	−2.81	−3.04	0.58
NMP	−0.26	−3.40	−2.87	−3.05	0.53
DMSO	−0.20	−3.20	−2.85	−3.07	0.44

*PC = propylene carbonate, MeCN = acetonitrile, EtOH = ethanol, DMF = *N*,*N*-dimethylformamide, NMP = *N*-methylpyrrolidone, DMSO = dimethyl sulfoxide.

For example, in the case of $n = 2$, $\Delta E^{\circ\prime}$ is calculated to be −35.6 mV at 298 K, which is a specific point that the current transient curves exactly increase twofold from the case of one-electron reaction, i.e. the system of two-step one-electron reaction behaves like one-electron reaction with 2 times of the bulk concentration.[18,19]

2.2 Metal reference/counter electrodes

Various metals are also applied as reference electrodes for systems utilizing metal ions as charge carriers because these systems often allow the reversible electrochemical deposition/dissolution of metals as follows:

$$M^{n+} + ne^- \rightleftharpoons M \tag{10}$$

Unlike the Ag reference electrode, there are no reference electrolytes separated by porous glass, indicative of environments uncontaminated by foreign chemical species such as Ag^+ and solvents existing only in the reference electrolytes. In systems that exhibit extremely high reversible M^+/M redox behavior, evaluation methods using two-electrode configurations with metal counter electrodes are well established, especially in the field of battery research such as alkali metal-ion batteries. The utilization of two-electrode configurations is highly advantageous because simple coin-type cells are available with negligible overpotentials of the metal counter electrodes during operation.

Nevertheless, the handling of metal reference/counter electrodes largely affects the electrochemical behavior, leading to the misinterpretation of obtained results. In the case of the two-electrode configurations, since the degree of the overpotential of the metal counter electrodes changes with the temperature, the current density, and the scan rate of the potential (voltage), it is advisable to check the overpotential in the corresponding experimental conditions with symmetric M/M cells, as described in Part 1. In three-electrode cells with metal reference electrodes, most electrolytes including alkali metal-ion systems provide relatively stable electrode potentials that are sufficient for electrochemical measurements. However, some systems show poor reversibility and large overpotentials of the metal deposition/dissolution reactions due to the formation of passivating films, leading to the instability of the counter/reference electrode potentials. Even in the reversible alkali metal-ion systems, the surface film, referred to as the "solid electrolyte interphase (SEI)", is formed on the alkali metal counter/reference electrodes, and their potentials shift from the ideal values because most electrolytes are intrinsically (thermodynamically) unstable toward the highly reactive alkali metal electrodes. In addition, the interfacial resistance of alkali metals usually increases with an increase in the period of contact with electrolytes.[20] Since the degree of the potential deviation depends on the stability of the electrolyte components, it is preferable to measure the potential difference between fresh and old metals and evaluate the surface resistance by impedance spectroscopy.

Research and development activities of post-lithium-ion batteries such as sodium-ion and potassium-ion ones are attracting increasingly more attention.[4,21–23] Most researchers discussed the latent capabilities of operating voltages based on the difference in famous alkali metal electrode potentials in aqueous solutions,[14,24] and they concluded that the expected operating voltage of sodium-ion batteries is 0.3 V smaller than that of lithium-ion batteries. However, the potential difference of 0.3 V can only be applied to aqueous solutions and is fundamentally different in nonaqueous systems. In general, the standard potentials of M^{n+}/M redox couples in nonaqueous systems can be converted from an aqueous system as follows:[14]

$$E^\circ(\text{non-aq}) = E^\circ(\text{aq}) + \frac{\Delta G_t^\circ}{nF} \tag{11}$$

where E°(non-aq) and E°(aq) are the standard potentials in nonaqueous and aqueous systems, respectively, and ΔG_t° is the standard molar Gibbs energy of ion transfer from aqueous to nonaqueous solutions. Table 1 lists the standard redox potentials of $H^+/\frac{1}{2}H_2$, Li^+/Li, Na^+/Na, K^+/K, and Ag^+/Ag in the selected solvents. Although these potentials were obtained using thermodynamic calculations according to Eq. 11 (not obtained by electrochemical measurements), they are strongly dependent on the solvent. In addition to the significantly large solvent dependence of $H^+/\frac{1}{2}H_2$ and Ag^+/Ag redox couples, the order of the potentials of the alkali metals changes among some organic solvents, for example, $E^\circ(K^+/K) < E^\circ(Li^+/Li) < E^\circ(Na^+/Na)$ in PC and acetonitrile, and $E^\circ(Li^+/Li) < E^\circ(K^+/K) < E^\circ(Na^+/Na)$ in water and some organic solvents. According to empirical knowledge, in the case of molten salts and ionic liquids, the K^+/K potential is often more negative than the Li^+/Li potential. A recent electrochemical assessment of alkali metal redox potentials in ionic liquid electrolytes revealed that the $E^\circ(K^+/K)$ value is more negative than that of $E^\circ(Li^+/Li)$ by approximately 0.2 V and the $E^\circ(Na^+/Na)$ value is more positive by only 0.1 V.[25,26] Thus, the potential difference between Li^+/Li and Na^+/Na is rather small to be less disadvantageous for constructing high-voltage sodium-ion batteries.

2.3 Advanced reference/counter electrodes

The electrode potential is a key metric for evaluating electrode materials for electrochemical measurements. As described in Sections 2.1 and 2.2, for nonaqueous systems, Ag and ferrocene reference electrodes are often used in a three-electrode configuration, and alkali metal reference electrodes are used in two-electrode cells (mostly coin cells) (Fig. 2). These two different cell configurations have clear advantages and disadvantages (see Section 2.4 in Part 1 for details about the three-electrode cell); for example, the potential of the reference electrode in the three-electrode cell is practically constant, whereas that in the two-electrode cell is not. Nevertheless, for the sake of convenience, the

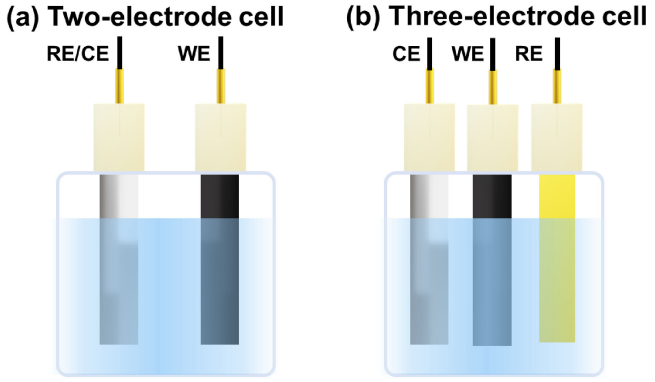

Figure 2. Schematic illustrations of (a) two-electrode cell and (b) three-electrode cell configurations for electrochemical measurements.

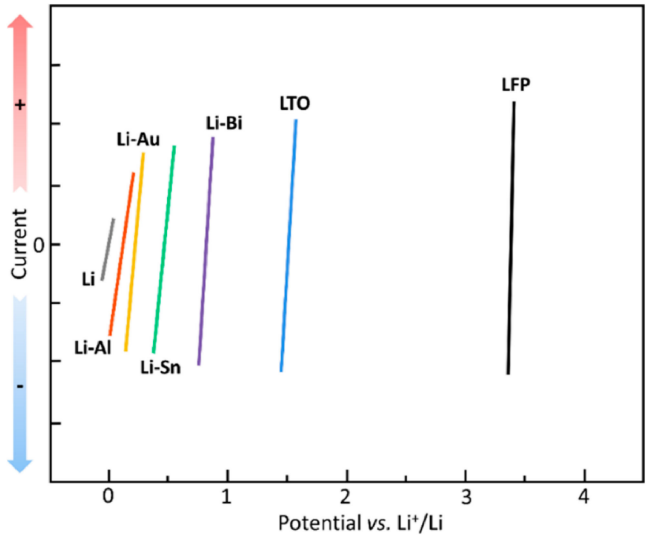

Figure 3. Comparison of potentials and polarization for Li, alloy materials, and advanced reference electrodes for lithium-ion batteries. Reproduced with permission under the Creative Commons Attribution License (CC BY).[28]

two-electrode cell is often selected for the study of batteries. However, alkali metals used as reference electrodes can cause problems and are far from the ideal reference electrode under certain conditions. These references frequently exhibit high reactivity toward electrolytes, which may cause a shift from the ideal potential by forming a passivation layer on the surface of the alkali metals, and the overpotential is amplified as the current density increases. Moreover, the experimental temperature ranges are restricted by the melting point of metals (Li: 179 °C, Na: 97.8 °C, K: 63.7 °C).[27]

In this regard, alternative reference electrodes using metal alloys and two-phase insertion-type compounds are attracting attention. The potentials of alternative reference electrodes for lithium-ion batteries are summarized in Fig. 3.[28] Metal alloy materials of Li–Sn, Li–Al, Li–Bi, and Li–Au were selected in some studies.[29–33] Their potentials are relatively more stable than those of alkali metals during electrochemical measurements for reasonable periods. These metal alloy references are often used for electrochemical impedance spectroscopy and potentiometry in lithium-ion and solid-state batteries (see Section 3.2). However, additional lithiation processes are necessary for these metal alloys to maintain a stable chemical composition. Furthermore, the temperature, current densities, and durations for alloy formation also strongly influence both the chemical composition and surface morphology of the metal alloy.[28,34] Thus, attempts have been made to use the equilibrium state of two-phase insertion-type compounds such as olivine $LiFePO_4$, spinel $Li_4Ti_5O_{12}$, and NASICON $Na_3V_2(PO_4)_3$.[34–38] These materials with flat plateaus during charge–discharge are considered suitable for use as reference electrodes.

The flat potential in a two-phase electrochemical transition can be derived from the Gibbs energy as follows. According to the Nernst equation described in Part 1, the voltage (V) of an electrochemical cell (half cell with Li metal counter electrode) of lithium-ion battery is related to the chemical potential, as shown in Eq. 12:[39,40]

$$V = -\frac{\mu_{Li} - \mu_{Li}^{metal}}{e} \tag{12}$$

where μ_{Li}^{metal} (eV per Li atom) is the Li chemical potential of the Li metal atom, which remains constant during electrochemical measurement (Li metal is used as a reference/counter electrode), μ_{Li} (eV per Li atom) is the Li chemical potential at each phase in two-phase insertion-type compounds, and e is the magnitude of the electron charge. The μ_{Li} is equal to the derivative of the Gibbs energy (g for per formula unit) with respect to the Li concentration (x) (e.g., x in Li_xFePO_4) according to Eq. 13:[39,40]

$$\mu_{Li} = \frac{\partial g}{\partial x} \tag{13}$$

The two phases (Li-poor α and Li-rich β phases) exhibit two local minima in the g–x plot. The μ_{Li} value is determined by the slope of the common tangent to the free energies of the α and β phases, which is consistent with the equivalent chemical potentials of the two phases in the equilibrium state (Fig. 4a).[39,40] Consequently, the voltage profiles of the two-phase transition compounds exhibit a flat plateau during charge–discharge, as shown in Figs. 4b and 4c.

Thus, the flat plateau region associated with a two-phase transition during the Li- or Na-ion insertion/desertion processes could behave as a nonpolarizable electrode with a small overpotential (Fig. 4c for the $Na_3V_2(PO_4)_3$–$NaV_2(PO_4)_3$ electrode as an example).[35] Although there are several attractive points for such reference electrodes, a practical drawback is the preparation of a partially charged state of these materials. These materials must be charged first to obtain the two-phase state to reach the flat plateau region. Thus far, the electrochemical method (charge in a half-cell configuration) has been applied to reach the partially charged state. However, the electrochemical process is time-consuming and unsuitable for mass production. Recently, an oxidation process was conducted using Cl_2 gas to extract Na^+ from $Na_3V_2(PO_4)_3$. This method does not harm the morphology of pristine materials and is suitable for mass production. Electrochemical measurements were carried out using a $Na_3V_2(PO_4)_3$–$NaV_2(PO_4)_3$ two-phase (3.4 V Na^+/Na) counter electrode combined with working electrode materials of $Na_2FeP_2O_7$, $Na_3V_2(PO_4)_3$, $NaCrO_2$, and hard carbon in organic and ionic liquid electrolytes. The $Na_3V_2(PO_4)_3$–$NaV_2(PO_4)_3$ electrode presented an accurate charge–discharge potential of the working electrodes even at high temperatures (>100 °C) at which Na metal melts. Moreover, the $Na_3V_2(PO_4)_3$–$NaV_2(PO_4)_3$ electrode exhibited high electrochemical stability during long cycles and low polarization compared with the Na metal electrode.

Computational methods can also be used to calculate an electrode potential based on the basic principle that the equilibrium voltage difference between positive and negative electrodes depends on the difference in their Li chemical potentials, as shown in Eqs. 12 and 13. Density functional theory (DFT) calculations have demonstrated that the electrode potentials for alkali metal batteries can be calculated from the change in the total energy.[41,42] For example, the electrode potential of $LiCoO_2$ vs. Li^+/Li can be calculated from Eq. 14.

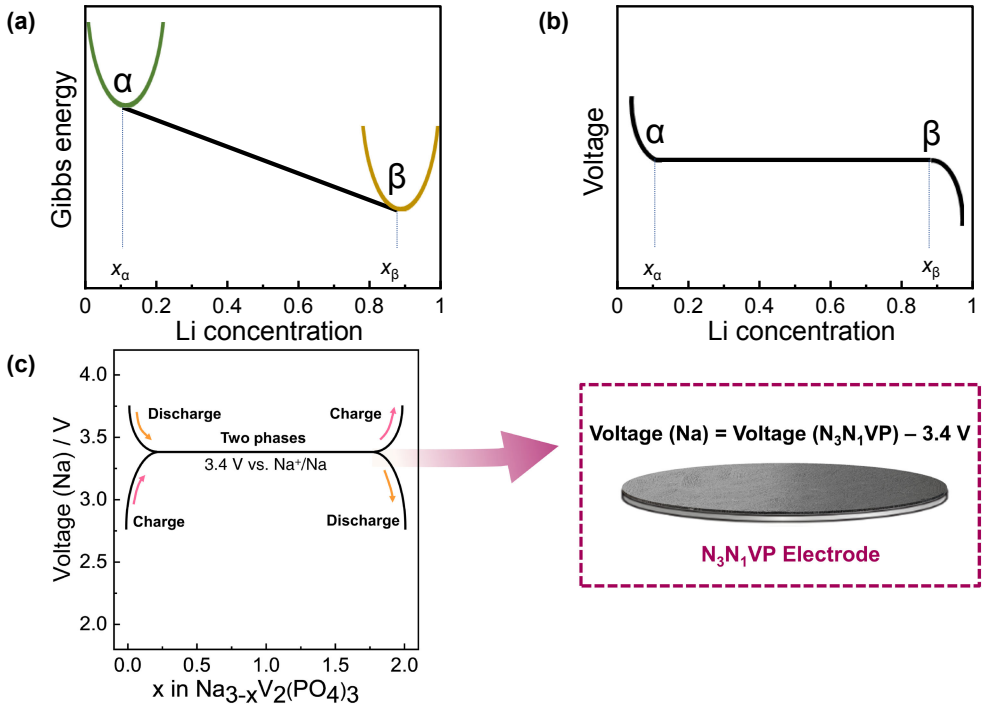

Figure 4. (a) Gibbs energy and (b) voltage profiles of two-phase transition materials. (c) Concept of pseudo reference/counter electrode utilizing the flat plateau of two-phase transition materials of $Na_3V_2(PO_4)_3$–$NaV_2(PO_4)_3$. Reproduced with permission.[35] Copyright 2021, Royal Society of Chemistry.

$$V = -\frac{[E_{LiCoO_2} - E_{Li_{(1-n)}CoO_2} - nE_{Li}]}{n} \quad (14)$$

where E is the total energy calculated from the DFT and n is the number of Li atoms extracted from $LiCoO_2$. The equilibrium electrode potential vs. Li^+/Li is obtained by calculating the difference in the total energies of the electrode active materials before and after Li extraction. When the structure (lattice parameter) varies with Li insertion or extraction, the difference in the total energies also varies with the composition. Thus, the electrode potential gradually shifts with a change in the composition. On the other hand, when a two-phase coexistence reaction occurs, as shown in Fig. 4b, the difference in the total energies is constant.

3. Solid-state Systems

3.1 All-solid-state batteries

All-solid-state batteries consist of only solid components. Solid electrolytes are expected to have various advantages, including high power, improved safety, and long lifetimes. As a representative solid-state system, this section outlines the basics of all-solid-state batteries, reference electrodes, and potential-window measurements of solid electrolytes.

Figure 5 shows a schematic of the structure of an all-solid-state lithium-ion battery. The battery has a layered structure consisting of a positive electrode current collector, positive electrode composite layer, separator layer (solid electrolyte layer), negative electrode composite layer, and negative electrode current collector. The positive electrode composite consists of a positive electrode active material, a solid electrolyte, a binder, and a conductive additive. Similarly, the negative electrode composite consists of a negative electrode active material, a solid electrolyte, a binder, and a conductive additive. The active material stores electricity through oxidation and reduction via Li extraction and insertion, respectively.

Positive electrode active materials used commonly are $LiCoO_2$ with a layered structure and Li(Ni, Mn, Co, Al)O_2 in which Co in

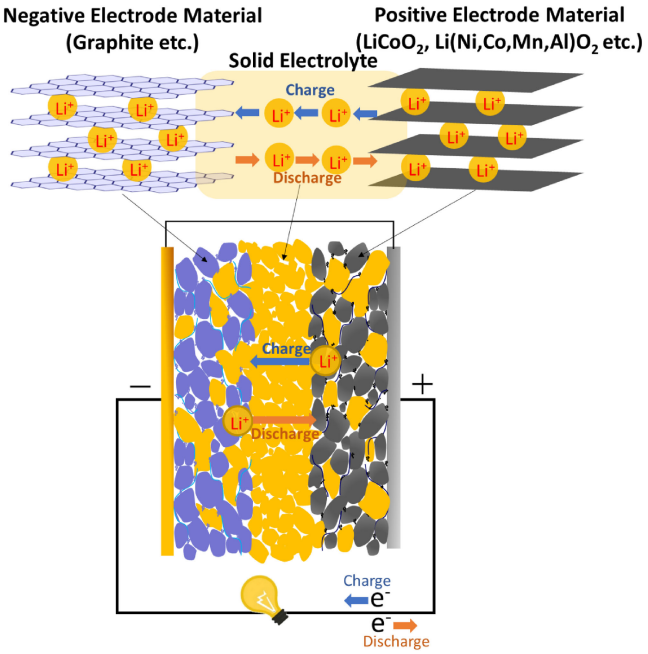

Figure 5. Schematic illustration of an all-solid-state battery.

$LiCoO_2$ is partially replaced with Ni, Mn, and Al.[43] $LiCoO_2$, Li(Ni, Mn, Co, Al)O_2, and $LiMn_2O_4$[44] are 4 V class electrode active materials, and $LiFePO_4$ is 3.5 V class.[45] Research and development of 5 V class high-potential materials and sulfur-based positive electrode active materials, which are 2 V class materials but enable a significantly large capacity, are being actively conducted. Graphite is the most commonly used negative electrode active material. Other materials that can be used as negative electrode active materials include hard carbon, spinel $Li_4Ti_5O_{12}$,[46] silicon, and tin, which form alloys with Li.

Solid electrolytes are key materials for all-solid-state batteries. The requirements that should be satisfied as solid electrolytes for this purpose are listed below.

(a) High ionic conductivity
(b) Low electronic conductivity
(c) High Li transference number $\sigma_{Li}/\sigma_{total}$ close to 1, where σ_{Li} is the Li-ion conductivity and σ_{total} is the conductivity contributed by all charge carriers (electron and all ions)
(d) High electrochemical stability at high and/or low potentials
(e) High chemical stability with positive and/or negative electrode materials and current collectors
(f) High press formability to construct an intimate contact interface between particles
(g) Low flammability, toxicity, and cost

Ideally, solid electrolytes that satisfy all the above requirements should be developed. In contrast, unlike liquid systems, different solid electrolytes can be used in the positive and negative electrode composite layers and in the solid electrolyte separator layer of solid systems. Typical sulfide electrolytes include $Li_{10}GeP_2S_{12}$ (LGPS),[47] argyrodite Li_6PS_5Cl,[48] and Li_3PS_4-based glass and glass ceramics,[49–51] whereas typical oxide electrolytes include $Li_{0.34}La_{0.51}TiO_{2.94}$,[6] $Li_{1.3}Al_{0.3}Ti_{1.7}(PO_4)_3$,[52] and $Li_7La_3Zr_2O_{12}$ (LLZ).[8] $Li_{3.3}PO_{3.8}N_{0.22}$,[53] Li_3BO_3-based glass, and glass ceramics[54,55] are also used for thin-film or small batteries. Halide electrolytes and complex hydrides have also attracted attention.[56–58] Sulfide, halide, and complex hydride electrolytes are generally characterized by high conductivity and excellent formability. Oxide-based electrolytes, on the other hand, basically have high chemical stability.

Most inorganic solid electrolytes show high Li transference numbers $\sigma_{Li}/\sigma_{total}$ close to 1. In solution systems, multiple ions, such as cations and anions, exist in the solvent, but solid electrolytes are often single-ion conductors in which only the carrier ions move. The electrochemical behavior can be interpreted in a simple manner because the carrier ion concentration changes very little in the electrolyte.

3.2 Electrode potential and reference electrode in all-solid-state batteries

It is necessary to fabricate a three-electrode electrochemical cell to accurately measure the electrode potentials. Detailed analysis requires investigation of the potential of each positive and negative electrode. However, the fabrication of a three-electrode cell in a solid-state system is more difficult than that in a liquid system. Thus, most electrochemical tests of all-solid-state batteries are performed in two-electrode configurations. As described above (Section 2.3), the electrode potential of solid solution reagion gradually shifts with a change in the composition. On the other hand, that of two-phase coexistence region shows constant voltage. Therefore, electrode active materials with two-phase coexistence reactions are useful as reference electrodes because they exhibit a constant voltage.

Li metal is typically used as the reference electrode for lithium-ion batteries. Although the Li metal electrode is the simplest counter/reference electrode in all-solid-state batteries, short-circuiting and electrolyte reductive decomposition can occur; thus, a more stable counter/reference electrode for the two-electrode configuration is needed.

Li–In alloys are mainly used as counter/reference electrodes in all-solid-state lithium batteries using sulfide-based solid electrolytes,[12,59] because they have a high Li diffusion coefficient and a constant potential (0.62 V vs. Li^+/Li) over a wide composition range owing to the two-phase coexistence region between In and LiIn. Figure 6 shows the initial discharge curve of the all-solid-state Li/In cell using a sulfide solid electrolyte. A constant voltage plateau is observed at 0.62 V vs. Li electrode for the wide composition range of $x = 0$–1 in Li_xIn.

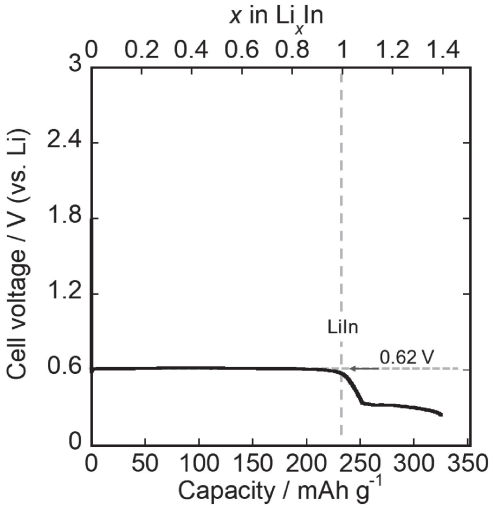

Figure 6. Discharge curve of the all-solid-state Li/In cell, exhibiting the two-phase coexistence region.

Furthermore, the resistance of the interface between the electrode and electrolyte for the Li–In electrode is relatively small in most cases. The relatively high electrode potential effectively suppresses the short-circuiting caused by Li dendrites, and thus acts as a stable counter electrode. More practically, it is recommended that Li_xIn be used within the composition range of $x = 0.2$ and 0.8. Li–In alloy foils can be obtained simply by overlapping and pressing a Li metal foil and an In metal foil because Li–In alloys have high Li diffusion coefficients. The key to successful alloying is the removal of impurities from the Li and In metal surfaces and holding them under pressure for a period of time. Similarly, $Li_4Ti_5O_{12}$ in the two-phase range is also useful as a counter/reference electrode in the same way.

In a three-electrode system for a lithium-ion battery using a liquid electrolyte, a Li wire or ribbon electrode located between the working and counter electrodes is typically used as the third electrode, as shown in Fig. 2. Although it is not easy to construct three-electrode cells similar to liquid systems for all-solid-state batteries, researchers have reported three-electrode cells for the characterization of all-solid-state batteries.[36,60,61]

In lithium-ion battery research, there is a great need to measure the potential and polarization (resistance) of the positive and negative electrodes using three-electrode cells to identify the dominant factors limiting the battery performance and the degradation sites. For example, Ikezawa et al. prepared an all-solid-state three-electrode cell using a chemically reduced $Li_4Ti_5O_{12}$ reference electrode for impedance analysis. For the shapes and locations of the reference electrodes, they chose mesh-type reference electrodes and positioned them between the positive and negative electrodes to reduce artifacts in the electrochemical impedance spectroscopy data.[36]

3.3 Electrochemical window of solid electrolytes

DFT calculations have clearly shown that most solid electrolytes are not thermodynamically stable against Li metal and are reduced at low potentials.[62] For example, the thermodynamically stable potential range for many sulfide-based solid electrolytes is very narrow, lying between 1.5–2.5 V vs. Li^+/Li. However, many of them can be used with both 4 V class positive electrode materials and 0–1 V class negative electrode materials. Figure 7 shows the cyclic voltammogram of an all-solid-state $Li/Li_7P_3S_{10}O$/stainless steel (SS) cell. The cell shows a relatively large current of Li plating/stripping at 0 V vs. Li^+/Li, and there is no large current even at 10 V vs. Li^+/Li. Although this result does not strictly mean

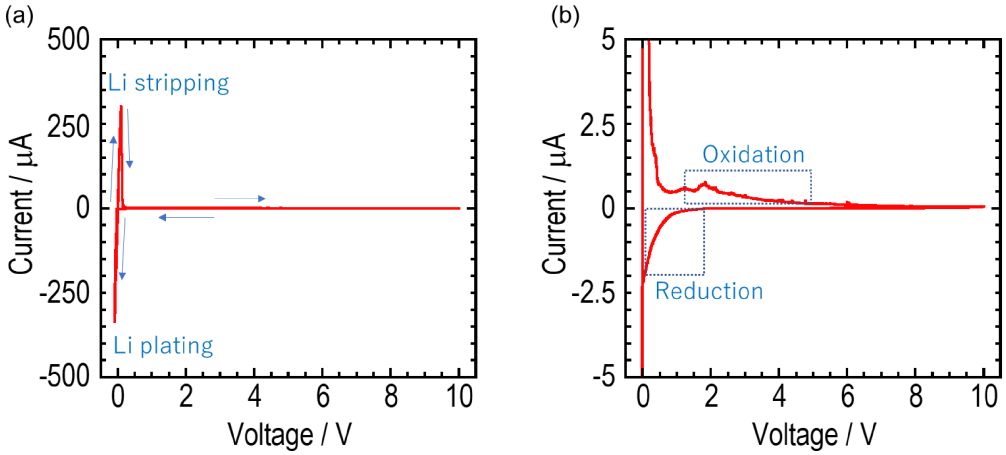

Figure 7. Cyclic voltammogram of the all-solid-state Li/$Li_7P_3S_{10}O$/SS cell. (b) shows magnified figure of (a).

that the solid electrolyte has an electrochemical window over a wide range of 0–10 V, it clearly indicates that this solid electrolyte could be used over a wide range of potentials. In contrast to liquid electrolytes, large oxidation and reduction currents often do not flow in the solid electrolytes. This is because oxidative decomposition does not occur continuously when the products of oxidative or reductive decomposition have low electronic conductivities. Non-flowability also contributes to the suppression of continuous oxidation and reduction currents due to side reactions. As shown in Fig. 7b, the anodic and cathodic currents due to the oxidation and reduction of the solid electrolyte observed at approximately 2 V vs. Li^+/Li are small, and the value is approximately 1/100 of the current density observed in Li plating/stripping. When the oxidation or reduction reaction products have very low electronic conductivities, the solid electrolyte does not undergo further decomposition. In addition, when the oxidation or reduction reaction products also have sufficient ionic conductivity, the all-solid-state battery works well, even though the solid electrolyte itself is thermodynamically unstable under high or low voltages. Instead of the self-forming oxidative and reductive decomposition layers, it is effective to introduce a buffer layer with very low electronic conductivity and high ionic conductivity in advance. It has been found that such a coating on the surface of the electrode active material particles can significantly reduce the resistance of the interface between the electrode and electrolyte.[12,63] The difference of chemical potential of Li between electrodes and solid electrolytes should be an important factor to understanding the side reaction and interfacial resistance.

4. Summary

Electrochemistry has progressed tremendously over the past several decades. The evaluation of the electrode potential is, in essence, the foundation of electrochemistry, as well as the key to developing electrochemical applications. In this Part 2, a summary of several reference electrodes and the methodologies and strategies for measuring the electrode potential in nonaqueous and solid electrolytes, thereby providing further insight into the nature of the electrode potential. The electrode potential is not only required for the development of new materials for electrochemical applications at the lab scale but also must be considered in the production stage. Thus, we believe that this literature will serve as a useful guideline and strategy that can be directly utilized to develop devices.

CRediT Authorship Contribution Statement

Jinkwang Hwang: Writing – original draft (Lead)
Takayuki Yamamoto: Writing – original draft (Lead)
Atsushi Sakuda: Writing – original draft (Lead)
Kazuhiko Matsumoto: Writing – review & editing (Supporting)
Kohei Miyazaki: Writing – review & editing (Supporting)

Data Availability Statement

The data that support the findings of this study are openly available under the terms of the designated Creative Commons License in J-STAGE Data listed in D1 of References. The authors' profiles of this paper can be found on the preface.[64]

Conflict of Interest

The authors declare no conflict of interest in the manuscript.

References

D1. J. Hwang, T. Yamamoto, A. Sakuda, K. Matsumoto, and K. Miyazaki, *J-STAGE Data*, https://doi.org/10.50892/data.electrochemistry.21357846, (2022).
1. G. Wang, Z. Lu, Y. Li, L. Li, H. Ji, A. Feteira, D. Zhou, D. Wang, S. Zhang, and I. M. Reaney, *Chem. Rev.*, **121**, 6124 (2021).
2. E. Fan, L. Li, Z. Wang, J. Lin, Y. Huang, Y. Yao, R. Chen, and F. Wu, *Chem. Rev.*, **120**, 7020 (2020).
3. Y. Zheng, D. Wang, S. Kaushik, S. Zhang, T. Wada, J. Hwang, K. Matsumoto, and R. Hagiwara, *EnergyChem*, **4**, 100075 (2022).
4. K. Matsumoto, J. Hwang, S. Kaushik, C.-Y. Chen, and R. Hagiwara, *Energy Environ. Sci.*, **12**, 3247 (2019).
5. T. Yamamoto, A. Yadav, and T. Nohira, *J. Electrochem. Soc.*, **169**, 050507 (2022).
6. Y. Inaguma, C. Liquan, M. Itoh, T. Nakamura, T. Uchida, H. Ikuta, and M. Wakihara, *Solid State Commun.*, **86**, 689 (1993).
7. K. Yamamoto, S. Yang, M. Takahashi, K. Ohara, T. Uchiyama, T. Watanabe, A. Sakuda, A. Hayashi, M. Tatsumisago, H. Muto, A. Matsuda, and Y. Uchimoto, *ACS Appl. Energy Mater.*, **4**, 2275 (2021).
8. R. Murugan, V. Thangadurai, and W. Weppner, *Angew. Chem., Int. Ed.*, **46**, 7778 (2007).
9. J. Fu, *Solid State Ionics*, **104**, 191 (1997).
10. J. Hwang, K. Matsumoto, C.-Y. Chen, and R. Hagiwara, *Energy Environ. Sci.*, **14**, 5834 (2021).
11. A. Miura, N. C. Rosero-Navarro, A. Sakuda, K. Tadanaga, N. H. H. Phuc, A. Matsuda, N. Machida, A. Hayashi, and M. Tatsumisago, *Nat. Rev. Chem.*, **3**, 189 (2019).
12. A. Sakuda, A. Hayashi, and M. Tatsumisago, *Chem. Mater.*, **22**, 949 (2010).
13. K. Izutsu, M. Ito, and E. Sarai, *Anal. Sci.*, **1**, 341 (1985).
14. Y. Marcus, *Pure Appl. Chem.*, **57**, 1129 (1985).
15. G. Gritzner and J. Kůta, *Electrochim. Acta*, **29**, 869 (1984).
16. A. J. Bard and L. R. Faulkner, *Electrochemical Methods: Fundamentals and Applications* (2nd ed.), Wiley & Sons, Inc., New York (2001).
17. R. S. Nicholson and I. Shain, *Anal. Chem.*, **36**, 706 (1964).
18. J. B. Flanagan, S. Margel, A. J. Bard, and F. C. Anson, *J. Am. Chem. Soc.*, **100**, 4248 (1978).
19. F. Ammar and J. M. Savéant, *J. Electroanal. Chem. Interfacial Electrochem.*, **47**, 215 (1973).
20. T. Hosokawa, K. Matsumoto, T. Nohira, R. Hagiwara, A. Fukunaga, S. Sakai, and K. Nitta, *J. Phys. Chem. C*, **120**, 9628 (2016).

21. N. Yabuuchi, K. Kubota, M. Dahbi, and S. Komaba, *Chem. Rev.*, **114**, 11636 (2014).
22. A. Eftekhari, Z. Jian, and X. Ji, *ACS Appl. Mater. Interfaces*, **9**, 4404 (2017).
23. T. Hosaka, K. Kubota, A. S. Hameed, and S. Komaba, *Chem. Rev.*, **120**, 6358 (2020).
24. S. G. Bratsch, *J. Phys. Chem. Ref. Data*, **18**, 1 (1989).
25. T. Yamamoto, K. Matsumoto, R. Hagiwara, and T. Nohira, *J. Phys. Chem. C*, **121**, 18450 (2017).
26. T. Yamamoto, S. Nishijima, and T. Nohira, *J. Phys. Chem. B*, **124**, 8380 (2020).
27. N. S. Gingrich and L. Heaton, *J. Chem. Phys.*, **34**, 873 (1961).
28. R. Raccichini, M. Amores, and G. Hinds, *Batteries*, **5**, 12 (2019).
29. J. L. Gómez-Cámer and P. Novák, *Electrochem. Commun.*, **34**, 208 (2013).
30. D. P. Abraham, S. D. Poppen, A. N. Jansen, J. Liu, and D. W. Dees, *Electrochim. Acta*, **49**, 4763 (2004).
31. H. Nara, D. Mukoyama, T. Yokoshima, T. Momma, and T. Osaka, *J. Electrochem. Soc.*, **163**, A434 (2016).
32. M. W. Verbrugge, D. R. Baker, and B. J. Koch, *J. Power Sources*, **110**, 295 (2002).
33. J. Landesfeind, D. Pritzl, and H. A. Gasteiger, *J. Electrochem. Soc.*, **164**, A1773 (2017).
34. F. La Mantia, C. D. Wessells, H. D. Deshazer, and Y. Cui, *Electrochem. Commun.*, **31**, 141 (2013).
35. J. Hwang, K. Takeuchi, K. Matsumoto, and R. Hagiwara, *J. Mater. Chem. A*, **7**, 27057 (2019).
36. A. Ikezawa, G. Fukunishi, T. Okajima, F. Kitamura, K. Suzuki, M. Hirayama, R. Kanno, and H. Arai, *Electrochem. Commun.*, **116**, 106743 (2020).
37. S. Yi, B. Wang, Z. Chen, R. Wang, and D. Wang, *RSC Adv.*, **8**, 18597 (2018).
38. J. Wandt, J. Lee, D. W. M. Arrigan, and D. S. Silvester, *Electrochem. Commun.*, **93**, 148 (2018).
39. D. Li and H. Zhou, *Mater. Today*, **17**, 451 (2014).
40. A. Van der Ven, J. Bhattacharya, and A. A. Belak, *Acc. Chem. Res.*, **46**, 1216 (2013).
41. M. S. Islam and C. A. J. Fisher, *Chem. Soc. Rev.*, **43**, 185 (2014).
42. M. K. Aydinol, A. F. Kohan, G. Ceder, K. Cho, and J. Joannopoulos, *Phys. Rev. B*, **56**, 1354 (1997).
43. T. Ohzuku and Y. Makimura, *Chem. Lett.*, **30**, 642 (2001).
44. R. J. Gummow, A. de Kock, and M. M. Thackeray, *Solid State Ionics*, **69**, 59 (1994).
45. A. K. Padhi, K. S. Nanjundaswamy, and J. B. Goodenough, *J. Electrochem. Soc.*, **144**, 1188 (1997).
46. T. Ohzuku, A. Ueda, and N. Yamamoto, *J. Electrochem. Soc.*, **142**, 1431 (1995).
47. N. Kamaya, K. Homma, Y. Yamakawa, M. Hirayama, R. Kanno, M. Yonemura, T. Kamiyama, Y. Kato, S. Hama, K. Kawamoto, and A. Mitsui, *Nat. Mater.*, **10**, 682 (2011).
48. H.-J. Deiseroth, S.-T. Kong, H. Eckert, J. Vannahme, C. Reiner, T. Zaiß, and M. Schlosser, *Angew. Chem., Int. Ed.*, **47**, 755 (2008).
49. A. Hayashi, S. Hama, T. Minami, and M. Tatsumisago, *Electrochem. Commun.*, **5**, 111 (2003).
50. Y. Seino, T. Ota, K. Takada, A. Hayashi, and M. Tatsumisago, *Energy Environ. Sci.*, **7**, 627 (2014).
51. A. Hayashi, S. Hama, H. Morimoto, M. Tatsumisago, and T. Minami, *J. Am. Ceram. Soc.*, **84**, 477 (2001).
52. H. Aono, E. Sugimoto, Y. Sadaoka, N. Imanaka, and G. y. Adachi, *J. Electrochem. Soc.*, **136**, 590 (1989).
53. J. B. Bates, N. J. Dudney, B. Neudecker, A. Ueda, and C. D. Evans, *Solid State Ionics*, **135**, 33 (2000).
54. M. Tatsumisago, R. Takano, K. Tadanaga, and A. Hayashi, *J. Power Sources*, **270**, 603 (2014).
55. M. Tatsumisago, N. Machida, and T. Minami, *Yogyo-Kyokai-Shi*, **95**, 197 (1987).
56. T. Asano, A. Sakai, S. Ouchi, M. Sakaida, A. Miyazaki, and S. Hasegawa, *Adv. Mater.*, **30**, 1803075 (2018).
57. M. Matsuo, Y. Nakamori, S.-I. Orimo, H. Maekawa, and H. Takamura, *Appl. Phys. Lett.*, **91**, 224103 (2007).
58. S. Kim, H. Oguchi, N. Toyama, T. Sato, S. Takagi, T. Otomo, D. Arunkumar, N. Kuwata, J. Kawamura, and S.-I. Orimo, *Nat. Commun.*, **10**, 1081 (2019).
59. K. Takada, N. Aotani, K. Iwamoto, and S. Kondo, *Solid State Ionics*, **86–88**, 877 (1996).
60. Y. J. Nam, K. H. Park, D. Y. Oh, W. H. An, and Y. S. Jung, *J. Mater. Chem. A*, **6**, 14867 (2018).
61. G. H. Chang, H. U. Choi, S. Kang, J.-Y. Park, and H.-T. Lim, *Ionics*, **26**, 1555 (2020).
62. Y. Zhu, X. He, and Y. Mo, *ACS Appl. Mater. Interfaces*, **7**, 23685 (2015).
63. N. Ohta, K. Takada, L. Zhang, R. Ma, M. Osada, and T. Sasaki, *Adv. Mater.*, **18**, 2226 (2006).
64. H. Yamada, K. Matsumoto, K. Kuratani, K. Ariyoshi, M. Matsui, and M. Mizuhata, *Electrochemistry*, **90**, 102000 (2022).